ELSEVIER

Biochimica et Biophysica Acta 1509 (2000) 385–396

BIOCHIMICA ET BIOPHYSICA ACTA
BBA

www.elsevier.com/locate/bba

The structure and thermotropic phase behaviour of dipalmitoylphosphatidylcholine codispersed with a branched-chain phosphatidylcholine

Konrad Semmler [a], Helmut W. Meyer [b], Peter J. Quinn [a,*]

[a] *King's College London, Division of Life Sciences, 150 Stamford Street, London SE1 8WA, UK*
[b] *Friedrich-Schiller University Jena, Institute of Ultrastructure Research, Ziegelmuehlenweg 1, 07743 Jena, Germany*

Received 25 April 2000; received in revised form 21 August 2000; accepted 24 August 2000

Abstract

The structure and thermotropic phase behaviour of a fully hydrated binary mixture of dipalmitoylphosphatidylcholine and a branched-chain phosphatidylcholine, 1,2-di(4-dodecyl-palmitoyl)-*sn*-glycero-3-phosphocholine, were examined using differential scanning calorimetry, synchrotron X-ray diffraction and freeze-fracture electron microscopy. The branched-chain lipid forms a nonlamellar phase when dispersed alone in aqueous medium. Mixed aqueous dispersions of the two phospholipids containing less than 33 mol% of the branched-chain lipid form lamellar phases over the whole temperature range were studied (4°C to 60°C). When present in proportions greater than 33 mol% it induces a hexagonal phase in mixed aqueous dispersions with dipalmitoylphosphatidylcholine at temperatures above the fluid phase transition. At temperatures below 35°C a hexagonal phase coexists with a gel bilayer phase. The lamellar↔nonlamellar transition can be explained satisfactorily on the basis of the shape of the molecule expressed in terms of headgroup and chain cross-sectional areas. At temperatures below 35°C macroscopic phase separation of two gel phases takes place. Freeze-fracture electron microscopy revealed that one gel phase consists of bilayers with a highly regular, periodic superstructure (macro-ripples) whereas the other phase forms flat, planar bilayers. The macro-ripple phase appears to represent a relaxation structure required to adapt to the packing constraints imposed by the incorporation of the branched-chain lipid into the dipalmitoylphosphatidylcholine host bilayer. The data suggest that structural changes that take place on cooling the mixed dispersion below the lamellar↔nonlamellar phase transition temperature cannot be adequately described using the molecular form concept. Instead it is necessary to take into account the detailed molecular form of the guest lipid as well as its physical properties.

Keywords: Branched-chain phospholipid; Freeze-fracture electron microscopy; Phospholipid; Ripple phase; Bilayer phase separation; Lipid packing

1. Introduction

Many biological membranes contain lipids with branched-chain fatty acids [1]. Particularly the iso and anteiso methyl-branched fatty acids are known to play a significant role in the growth of microorganisms [2]. By regulating the amount of these lipids, bacteria are able to maintain bilayer structures within a wide range of environmental temperatures [3].

Apart from a regulatory function, branched-chain

* Corresponding author. Fax: +44-207-848-4500; E-mail: p.quinn@kcl.ac.uk

0005-2736/00/$ – see front matter
PII: S0005-2736(00)00321-7

fatty acids create a lipid environment that directly effects the activation of peripheral and integral membrane proteins [4]. The molecular mechanisms of these interactions are often unclear, however it has been suggested that changes in the physical state of the lipid bilayer may trigger protein conformational changes. In particular, lipids showing a propensity for nonlamellar structures like diacylglycerol or branched-chain species are believed to exert their effects by modifying the lipid bilayer in terms of fluidity and local curvature [5] or by packaging the protein into the lipid matrix [6].

The inherent property of branched-chain lipids to arrange in nonlamellar aggregates when dispersed in aqueous systems is well known. This is said to be due to a cone or wedge shape molecular form, in which the cross-sectional area of the chains exceeds the area of the headgroup thus favouring a micellar or a cubic rather than a lamellar phase state. The molecular form concept describes the tendency of a lipid system to form bilayer or nonbilayer phases by considering the ratio of headgroup and chain cross-sectional area of the constituent lipids [7,8]. The deviation of a molecular packing parameter $P = V_L/A_H \cdot l$ from unity then determines how likely the formation of a nonlamellar phase is [9]. Here V_L is the volume of the lipid molecule, A_H is headgroup cross-sectional area and l is the length of the molecule.

Model studies with single component branched-chain lipids have been reported by Lewis et al. [10] who showed that phosphatidylcholines with different substituents at the C2-position of the fatty acids have a general tendency to form nonlamellar phases. The influence of length of the branched chain on phase transition temperatures and thermotropic polymorphism was examined in model studies of phosphatidylcholines with branched side chains between 1 and 18 C-atoms long [11]. One interesting finding from this study was that the gel-to-liquid crystalline phase transition temperature showed a maximum for an intermediate chain length of about 12 C-atoms. Another feature particularly of short-branched lipids is the appearance of interdigitated gel phases [12].

In contrast to these one-component studies there are only few reports about binary mixtures of two components with defined geometry, despite the fact that such systems are ideal to obtain insight into structure formation principles in biological membranes. In this work we present a structural and thermal study of a mixture of dipalmitoylphosphatidylcholine with the branched-chain lipid 1,2-di-(4-dodecyl-palmitoyl)-*sn*-glycero-3-phosphocholine. The four-chain lipid differs from dipalmitoylphosphatidylcholine solely by having a 12 C-atom branch on the fourth C-atom of each main chain. The fully hydrated branched-chain lipid exhibits two phase transitions, a low-temperature transition at ~ -17.5°C between a lamellar crystal ($L_{c'}$) and a lamellar gel ($L_{\beta'}$) phase and a transition at ~ 3°C which resembles the formation of a nonlamellar, hexagonal fluid phase (H_{II}) [13]. The aim of this study was to establish principles of structure formation of lipid mixtures consisting of two components with a defined molecular form and well-known phase behaviour.

2. Materials and methods

2.1. Sample preparation

1,2-Dipalmitoyl-*sn*-glycerophosphocholine (DPPC) was purchased from Sigma (St. Louis, USA). 1,2-Di(4-dodecyl-palmitoyl)-*sn*-glycero-3-phosphocholine (4C12-PC16) was a gift of B. Dobner (University Halle-Wittenberg, Germany). The synthesis of the lipid has been described elsewhere [11]. Amounts of 20 mg of the lipids were dissolved in chloroform and mixed in appropriate proportions. A thin film of dry lipid was formed on the wall of a glass vessel by rotary evaporation under reduced pressure. The lipid film was subsequently stored for at least 6 h under vacuum to remove any remaining traces of solvent. Weighted amounts of bi-distilled water were added to the dry lipid to obtain multilamellar dispersions. The water content was adjusted to 60% (wt/wt). The lipid dispersions were hydrated at 60°C for 30 min, vigorously vortexed, stored at 4°C for 12 h and again heated to 60°C for 30 min. After this procedure the sample was stored at 4°C until required for examination.

2.2. Differential scanning calorimetry

Calorimetric measurements of the sample containing 50 mol% 4C12-PC16 were performed using a

Pyris 1 instrument (Perkin-Elmer, Newalk, USA) at a scan rate of 5°C/min. The sample was incubated at room temperature (22°C) for 24 h and then a heating scan from 22°C to 60°C followed by a cooling scan to −5°C and a successive heating scan to 60°C was recorded.

2.3. Simultaneous DSC and synchrotron X-ray diffraction measurements

Simultaneous DSC and synchrotron X-ray diffraction was performed at Station 8.2 of the Daresbury Synchrotron Laboratory (UK). The samples were incubated for at least 24 h at 4°C prior to measurement. The samples were placed in a standard 10 μl DSC alluminium pan (Perkin-Elmer, Newalk, USA) and sealed with a mica lid affixed to the rim of the pan. The sample holder was mounted in a modified Linkam cryostage equipped with a silver heat flow plate. A liquid nitrogen pump and a resistance heater combined with a precision DC temperature controller were used to drive cooling and heating scans. A reference signal was produced independently under identical conditions and used to calculate differential heat flow. Details of the combined DSC–X-ray diffraction set-up are described elsewhere [14].

The samples were heated to 60°C, cooled to 4°C and immediately reheated to 60°C with a scan rate of 5°C/min. The relatively high heating/cooling rates were employed so as to minimise the time of exposure of the samples to the high intensity X-ray beam. Under these conditions there was no evidence of any radiation damage to the sample. Separate experiments performed on selected samples prepared in sealed glass capillary tubes subjected to thermal scans of 0.1 to 0.5°C/min showed only minor differences in the onset of phase transitions ($\sim$1°C) judged from SAXS measurements. The width of the transitions, however, did depend on scan rate but this does not alter the essential conclusions that were drawn from the study. X-ray scattering patterns were recorded by measuring the intensity of scattered X-rays from the sample accumulated over 5 s corresponding to a temperature resolution of 0.4°C for each scattering profile. Frame averaging procedures were used to enhance the signal-to-noise ratio for graphical presentation. The applied averaging protocol is specified in the respective figure legends. Small-angle X-ray scattering (SAXS) intensity patterns were measured using a quadrant detector located at a distance of 2.3 m from the sample. Wide-angle X-ray scattering (WAXS) intensity profiles were measured with a curved INEL detector (Instrumentation Electronique, France). The INEL detector was spatially calibrated using the peaks from high-density polyethylene (0.4166, 0.3780 and 0.3014 nm) and the SAXS detector was calibrated using the first nine orders of wet rat-tail collagen (repeat distance 67.0 nm). Details of the SAXS and WAXS facilities have been published elsewhere [15]. SAXS and WAXS data were corrected for beam intensity fluctuations recorded using an ionisation chamber located on the incident beam side of the sample and for detector response. Detector response profiles were recorded from a ^{59}Fe source. WAXS intensity profiles were corrected for background scattering by subtracting the scattering profile obtained at 60°C, where the sample was in the fluid phase. This procedure was necessary because the low signal-to-noise ratio did not allow a background subtraction using a single measurement obtained from an empty cell. A further reason was that the sample pans contained impurities causing scattering peaks whose relative intensity varied strongly between different sample pans. The reflections corrected in this way were not used to index the WAXS peaks, to interpret the configuration of the chain tilt, etc.

A sample containing 60 mol% 4C12-PC16 was also examined using the small- and wide-angle X-ray diffraction facilities at Station X33 of the EMBL outstation at DESY (Hamburg, Germany). The camera length was 1.5 m. The SAXS detector was spatially calibrated using silver behenate (first-order peak 58.39 nm); the WAXS detector was calibrated using *p*-bromo-benzoic acid (0.564, 0.517, 0.468, 0.393, 0.380, 0.370 nm). The samples were sealed in 1 mm diameter glass capillary tubes and subjected to thermal scans at a rate of 2°C/min.

2.4. Freeze-fracture electron microscopy

Samples and tools used for sample manipulation were equilibrated at the desired temperature for at least 15 min. For cryofixation a small drop of the suspension was sandwiched between two copper plates and manually plunged into liquid propane.

Fracturing and shadowing were performed at −150°C in a BAF 400D freeze-etching device (Balzers, Liechtenstein). The replicas were cleaned with chloroform and examined using a CEM 902A (Zeiss, Germany) electron microscope.

3. Results

The experimental set-up of Station 8.2 of the Daresbury SRS provides a unique opportunity to record simultaneously thermal and structural data of the same sample in real time. Such an approach is especially valuable, because it eliminates problems arising from different sample preparations and any influence of the thermal history of the samples. The facility was used to examine mixed aqueous dispersions of DPPC and 4C12-PC16 to gain insight into the influence of amphipathic balance of the system on bilayer stability.

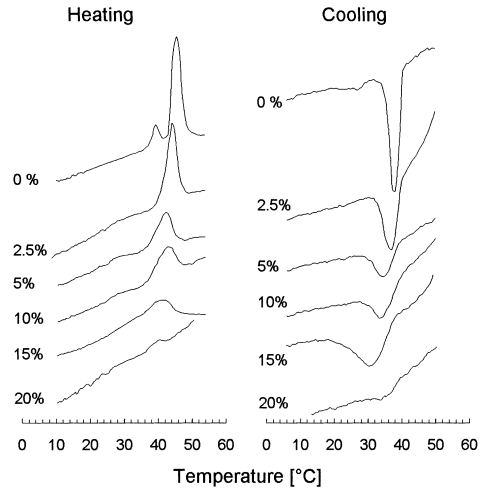

Fig. 1. Thermograms from mixtures of DPPC with up to 20 mol% of 4C12-PC16 recorded simultaneously with SAXS/WAXS data (see Figs. 2, 3) during a heating and cooling scan between 4 and 60°C at 5°C/min. The molar proportion of 4C12-PC16 is indicated.

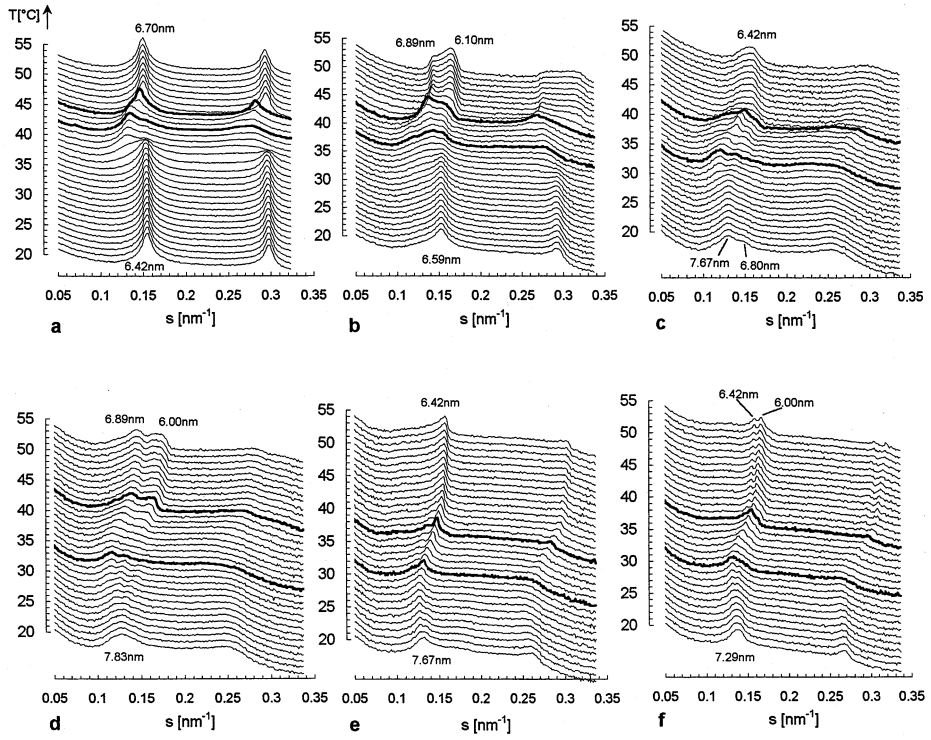

Fig. 2. SAXS intensity profiles recorded from mixtures of DPPC containing up to 20 mol% 4C12-PC16 obtained simultaneously with thermal (Fig. 1) and WAXS data (Fig. 3) during a heating scan from 4 to 60°C. (a) Pure DPPC. (b) 2.5 mol% 4C12-PC16. (c) 5 mol% 4C12-PC16. (d) 10 mol% 4C12-PC16. (e) 15 mol% 4C12-PC16. (f) 20 mol% 4C12-PC16. The profiles marked in bold represent SAXS intensities that correspond to the temperatures of the onset and peak, respectively, of the main thermal transition as detected by DSC (Fig. 1). For 15 and 20 mol% of the branched-chain lipid no DSC onset temperature could be detected; in these cases the start of the main transition was estimated by the onset of SAXS peak shifts towards higher angles. Temperature resolution: ~1°C.

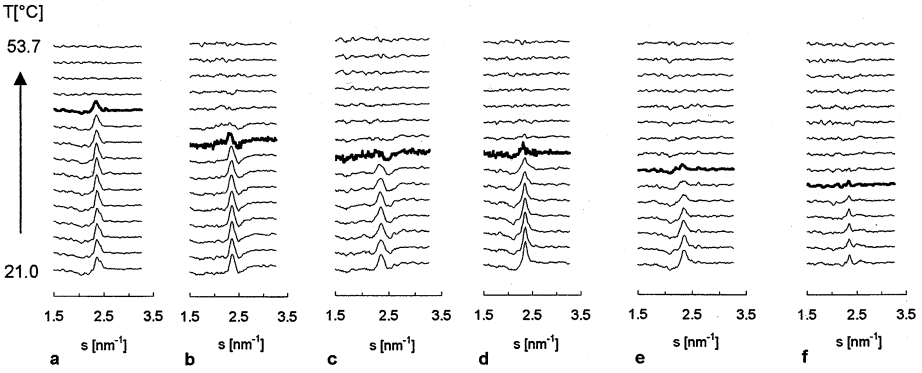

Fig. 3. WAXS intensity profiles recorded from mixtures of DPPC with up to 20 mol% 4C12-PC16 obtained simultaneously with thermal (see Fig. 1) and SAXS data (see Fig. 2) during a heating scan from 4 to 60°C. (a) DPPC. (b) 2.5 mol% 4C12-PC16. (c) 5 mol% 4C12-PC16. (d) 10 mol% 4C12-PC16. (e) 15 mol% 4C12-PC16. (f) 20 mol% 4C12-PC16. The marked profiles indicate the disappearance of the sharp diffraction peak from the ordered chains of gel phase bilayers. Temperature resolution: ~2°C.

Thermal (Fig. 1) and structural data (Figs. 2, 3) for heating and cooling scans of aqueous dispersions of DPPC containing up to 20 mol% of the branched-chain lipid, 4C12-PC16, were recorded. The heating scans show that the pretransition of DPPC, which is centred at 38°C, is greatly reduced in the presence of 2.5 mol% 4C12-PC16. In mixtures containing 15 and 20 mol% the pretransition can no longer be detected. The heating endotherms in Fig. 1 show that with increasing amounts of 4C12-PC16 lipid there is a broadening of the main transition together with a shift to lower temperatures. At 20 mol% of 4C12-PC16 the endothermic transition is almost abolished. The cooling exotherms provide an identical picture and show even more clearly the low-temperature shift and broadening of the thermal transition.

Small-angle X-ray scattering intensity recorded simultaneously with the data in Fig. 1 is presented in Fig. 2. Bold lines indicate the SAXS profiles corresponding to the onset and peak temperatures of the DSC heating endotherms shown in Fig. 1. The temperature range defined in this way resembles the coexistence region of fluid and gel phase bilayers. Two main effects can be seen in the pure gel phase region in each mixture which correspond to the temperature range below the region of phase coexistence: (1) A broadening of the reflections, most obvious for the 5 and 10 mol% sample, and (2) an increase of the lamellar repeat spacing from 6.42 nm for pure DPPC to 7.83 nm for mixtures containing 10 mol% branched-chain lipids with a subsequent decrease to 7.29 nm for the 20 mol% sample. The high-temperature range, where the mixture is entirely in the fluid state, also exhibits some unusual features. The samples containing 2.5, 10 and 20 mol% branched-chain lipid clearly show at least two sets of lamellar spacings at 6.89, 6.42 and 6.1/6.0 nm, respectively. The 5 and 15 mol% samples show broad peaks each suggesting a superposition of two closely aligned lamellar reflections.

The corresponding wide-angle X-ray scattering intensity patterns are shown in Fig. 3. The presence of a sharp reflection around 2.4 nm^{-1} indicates a gel phase with ordered chains. It is seen that with increasing concentrations of 4C12-PC16 the gel region is destabilised and the transition temperature decreases from 44.5°C for DPPC to about 34°C for

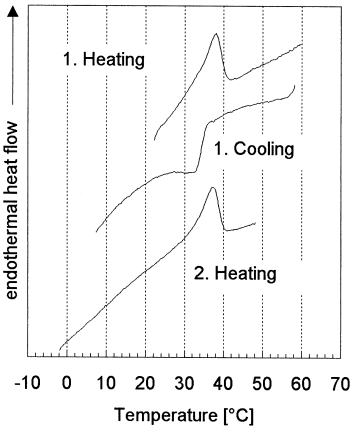

Fig. 4. Thermograms obtained from a mixed dispersion of DPPC containing 50 mol% 4C12-PC16. The sample was equilibrated at 22°C followed by heating to 60°C, a subsequent cooling to −5°C and a reheating to 60°C at a rate of 5°C/min.

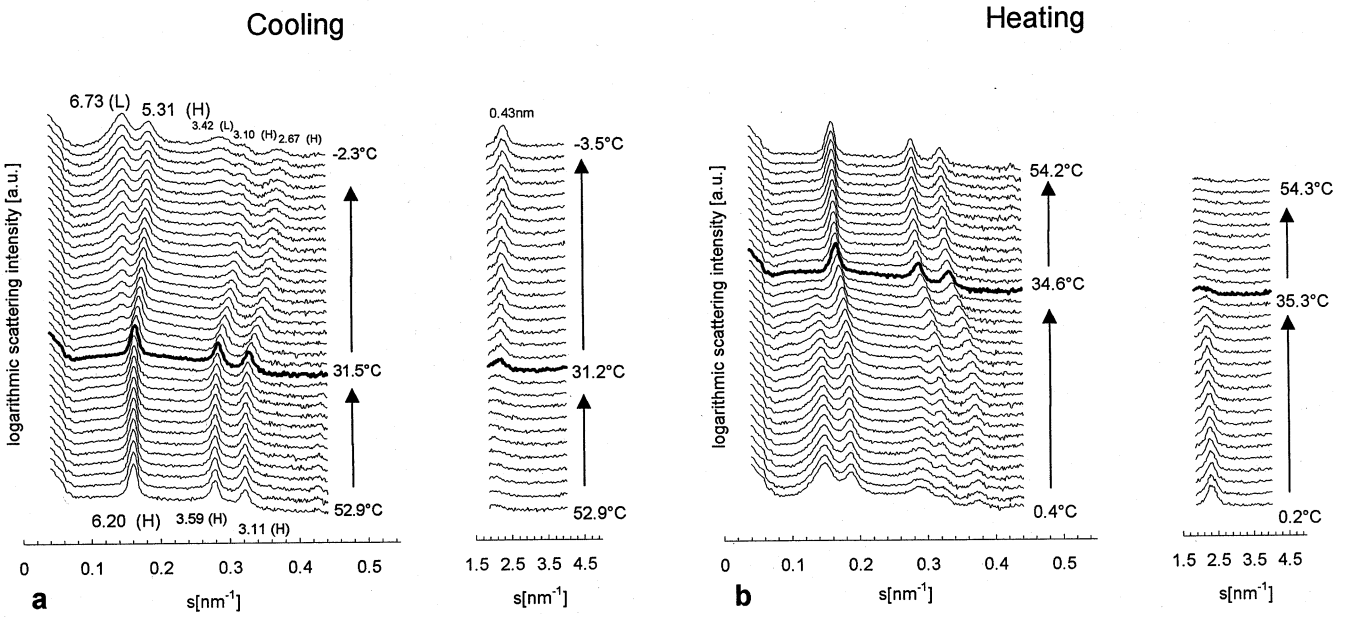

Fig. 5. Simultaneous SAXS/WAXS of a mixed aqueous dispersion of DPPC containing 60 mol% 4C12-PC16 recorded during (a) cooling and (b) reheating. SAXS intensity is plotted in a logarithmic scale with a temperature resolution per frame of ~1.6°C. The WAXS frames have a temperature resolution of ~1.9°C. The marked patterns indicate the approximate gel–fluid transition according to WAXS. SAXS peaks; labels denote long spacings in nm. H, hexagonal peak; L, lamellar peak.

the mixture containing 20 mol% branched-chain lipid. Additionally, this confirms that there is no gel phase at higher temperatures, which might coexist with a fluid phase, thereby creating the additional lamellar spacings seen in the SAXS experiments.

The general phase behaviour changed significantly for mixed dispersions containing more than 30 mol% 4C12-PC16. The transition enthalpies became so small that the on-line DSC device could not detect any thermal events. We therefore analysed these mixtures using conventional DSC. Fig. 4 shows thermograms of a sample of DPPC with 50 mol% 4C12-PC16 equilibrated at 22°C for 24 h. The first heating run shows a small thermal event with a peak temperature at around 38°C. On cooling, undercooling occurred with a hysteresis of about 4°C. No further thermal transition could be detected down to −5°C. The reheating scan mirrored the first heating scan. The structural changes associated with these transitions are presented in Fig. 5 showing simultaneous SAXS/WAXS experiments of a sample containing DPPC and 60 mol% 4C12-PC16. The left panel shows a cooling scan commencing from approximately 53°C. At this temperature the sample shows small-angle diffraction spacings in the order 1:1/v3:1/2 typical of a hexagonal phase. Upon cooling, at approx. 32°C, a gel phase begins to emerge as evidenced by the appearance of a sharp reflection in the wide-angle scattering region. Simultaneously the diameter of the hexagonally packed micelles becomes smaller evidenced by the shift of the reflections to higher angles. This shift is accompanied by the gradual appearance of additional reflections in the small-angle X-ray scattering range. The reflections can unambiguously index as a lamellar structure with a repeat spacing of 6.73 nm at about −2°C. The subsequent heating scan (right panel of Fig. 5) shows that these transitions are completely reversible. A slight temperature hysteresis of about 3°C can be observed.

Two questions remain after the X-ray diffraction experiments: (1) What is the reason for the remarkable peak broadening of the SAXS reflections in the 5 and 10 mol% samples at low temperatures? And (2), where do the multiple SAXS reflections in the fluid phase originate? To address these questions, we examined the equilibrium structure of the mixed dispersions using freeze-fracture electron microscopy.

The analysis of mixtures thermally quenched from

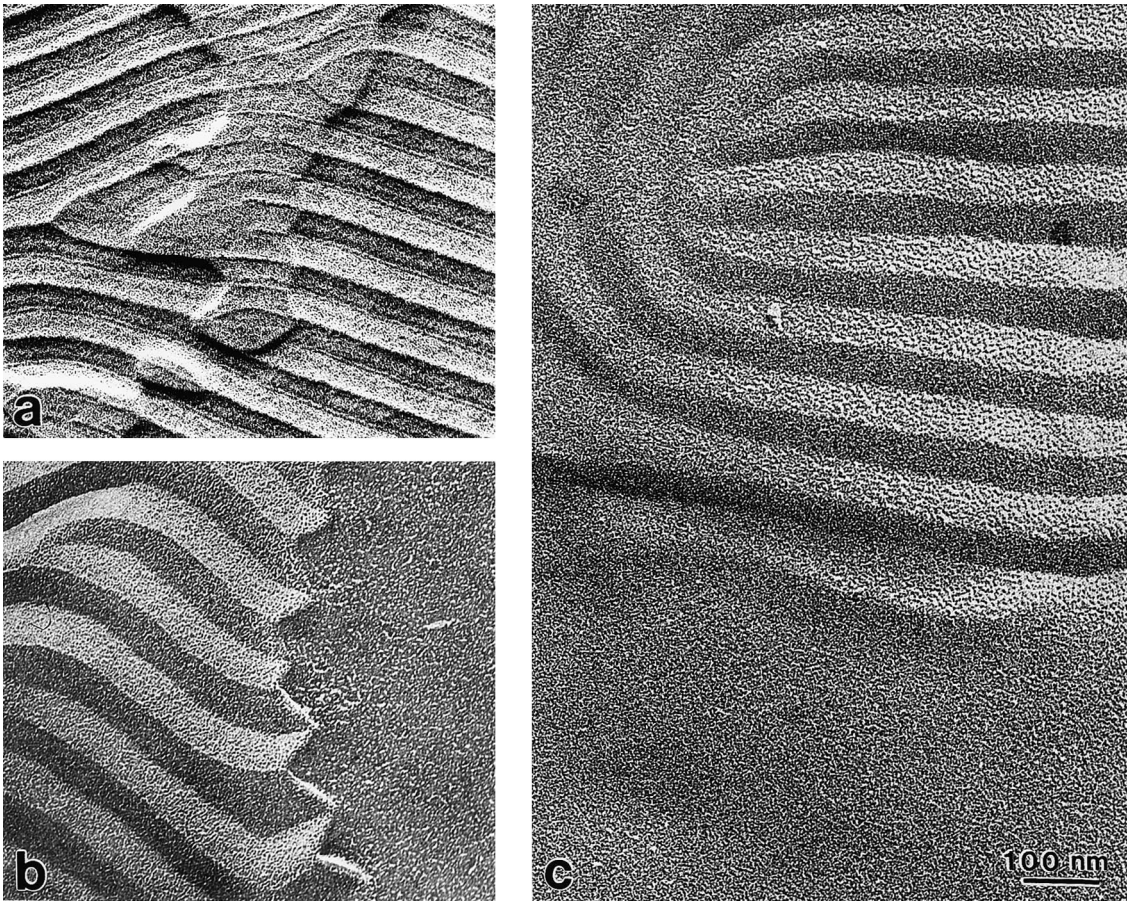

Fig. 6. Electron micrographs of freeze-fracture replicas prepared from aqueous dispersions of DPPC and 4C12-PC16 thermally quenched from the gel phase. (a) DPPC+10 mol% 4C12-PC16, 30°C. (b) DPPC+20 mol% 4C12-PC16, 4°C. (c) DPPC+20 mol% 4C12-PC16, 20°C. The samples were stored at 4°C for several days before rewarming to the respective temperatures where they were equilibrated for 30 min prior to thermal quenching. Scale bar corresponds to 100 nm.

the gel phase showed that for mixtures containing between 5 mol% and approx. 30 mol% of the branched-chain lipid rippled bilayers were formed which had unusually large periodicities (up to 120 nm). We refer to these ripples as macro-ripples and details of the characterisation of these macro-ripple phases have been published elsewhere [16]. Fig. 6 presents typical examples of these modulated bilayers. Fig. 6a shows that the large periodic modulation occurs via a periodic tilting of originally flat areas, which are subdivided by a line pattern. From Fig. 6b it becomes evident that single bilayers show the modulation, which excludes the possibility that interbilayer forces are responsible for this characteristic morphology. With increasing concentrations of 4C12-PC16 the relative proportion of bilayers showing these ripples decreased whereas flat membranes without the pattern became the dominant structure. Fig. 6c shows an example of coexisting rippled and flat bilayers, suggesting a macroscopic phase separation. At a concentration of approximately 2:1 (DPPC:4C12-PC16) all bilayers are flat. The macro-ripples were stable in the whole temperature range below the main transition. The broad multipeaks found in the gel phase, especially in samples containing 5 and 10 mol% of the branched-chain lipid, can therefore be attributed to scattering from the two-dimensional lattice of this macro-ripple phase.

In contrast to low-temperature experiments, freeze-fracture experiments from the liquid crystalline state are notoriously difficult to interpret due to the danger of phase changes during quenching through the main transition. Despite this problem, structures with relatively slow transition kinetics

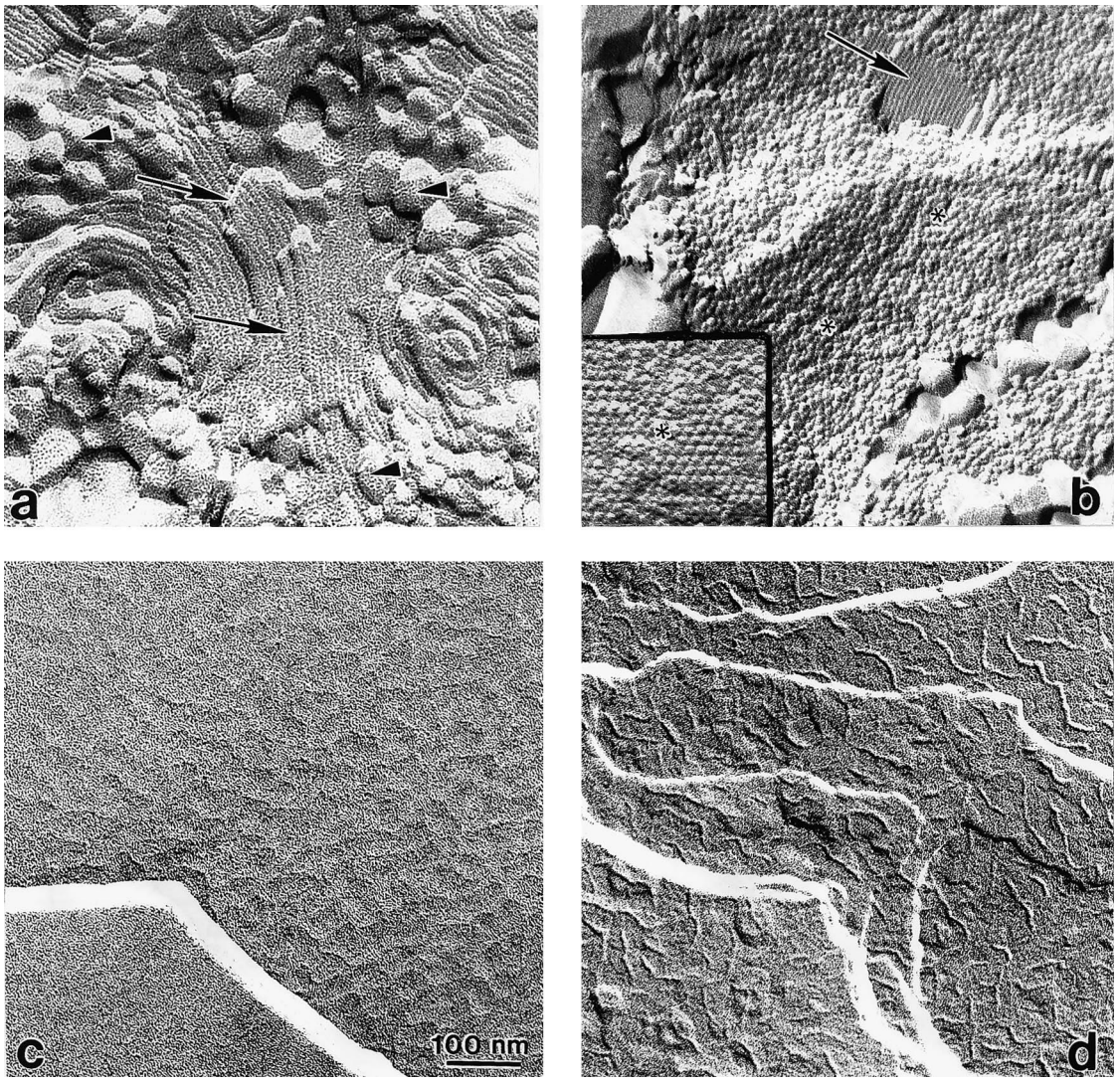

Fig. 7. Electron micrographs of freeze-fracture replicas prepared from aqueous dispersions of DPPC and 4C12-PC16 thermally quenched from the liquid crystalline phase. (a,b) DPPC+50 mol% 4C12-PC16, 40°C. Arrows indicate hexagonally packed cylindrical micelles. Arrow heads point to bilayer nucleation sites. Asterisks denote areas similar to densely packed spherical micelles. (c) DPPC+20 mol% 4C12-PC16, 40°C. (d) DPPC+5 mol% 4C12-PC16, 55°C. Scale bar corresponds to 100 nm.

like hexagonal and cubic phases may be successfully captured. This is demonstrated in Fig. 7a which shows a hexagonally packed array of cylindrical micelles (arrows) in a sample containing DPPC and 50 mol% 4C12-PC quenched from 40°C. The diameter of the cylinders is not constant throughout their length suggesting that during the freezing process changes in the composition of the micelles take place. In addition it can be seen that there are small areas with a flat appearance (asterisk) corresponding, presumably, to bilayer nucleation sites. In these samples, containing between ~30 and 60 mol% 4C12-PC16, we also frequently saw regions typical of cubic phases or at least similar to the appearance of densely packed spherical micelles together with hexagonally packed cylinders (Fig. 7b). In mixtures with lower proportions of 4C12-PC16 (below ~30 mol%) only lamellar structures could be found when quenched from above the coexistence region. However, the bilayers creating these lamellae often showed an irregular pattern as demonstrated in Fig. 7c,d.

4. Discussion

Three different questions must be considered to explain the structure of aqueous dispersions of binary lipid mixtures: (1) How does a second component change the phase transition temperature of the host lipid and does it eventually induce new phases? (2) Are there macroscopic phase separations, e.g. coexistence of two lamellar phases or demixing into a lamellar and a hexagonal phase? (3) Are there microscopic phase separations, which manifest as regular (periodic) superstructures, more or less irregular deformations of the (gel) bilayer? All three questions can be addressed in the binary system examined in the present study. In the following discussion we have attempted to identify the important parameters for the respective phases. The analysis commences with construction of a partial phase diagram of the binary system.

4.1. Partial phase diagram

Using the thermal and structural data from the simultaneous DSC/SAXS/WAXS measurements a partial phase diagram of the mixture of DPPC and 4C12-PC16 can be constructed (Fig. 8). The phase boundaries were determined primarily from the onset and peak temperatures of the heating endotherms. The electron microscopy data were used to identify ripple phases and H_{II} phases and to confirm two-phase regions evident by the presence of different bilayer topologies. In addition, the dynamic SAXS data allowed an unambiguous assignment of lamellar and hexagonal phases.

The phase diagram is characterised by two critical concentrations, dividing it into three regions:

1. Amounts of less than 5 mol% 4C12-PC16 are miscible with DPPC in both the gel and fluid phase. At temperatures below the main transition temperature a ripple phase is formed, which consists solely of symmetric ripples with a periodicity of approx. 25 nm.
2. Between 5 and ~33 mol% 4C12-PC16 a two-phase region is found at low temperatures: firstly, a gel phase (Gel_1) with one branched lipid per 19 DPPC molecules forms bilayers with a characteristic macro-ripple modulation. With increasing amounts of 4C12-PC16 the relative proportion of these bilayers decreases, whereas the proportion of flat bilayers shows a corresponding increase. These flat bilayers are formed by a second gel phase (Gel_2) which is composed of DPPC:4C12-PC16 2:1. At 33 mol% the sample consists entirely of Gel_2 phase. Upon heating from the two-phase region, the Gel_2 phase melts at around 35°C, whereas the Gel_1 phase remains solid until reaching the liquidus line of the phase diagram. At temperatures above the liquidus boundary a fluid lamellar phase is formed. The question whether this region consists of more than one lamellar phase is discussed below.
3. In mixtures containing more than ~33 mol% 4C12-PC16, another two-phase region is present at low temperatures. This arises, because the additional branched lipids cannot be incorporated into the Gel_2 bilayer; a separate phase ($_1H_{II}$) composed of almost pure 4C12-PC16 is formed. Heating mixtures in that concentration range result in a phase transition at around 35°C. At that temperature the Gel_2 bilayers melt and the lipids are incorporated into a single mixed, hexagonal phase $_2H_{II}$. It could be that this region is a two-phase

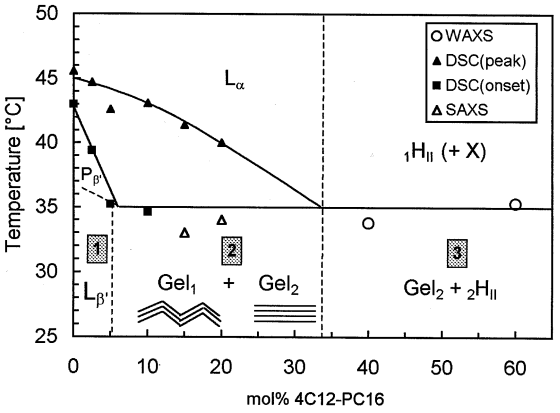

Fig. 8. Partial phase diagram of DPPC and 4C12-PC16. Phase boundaries were determined from the onset and peak temperatures of the DSC heating endotherms and from the onset temperatures of lamellar repeat shifts in real-time SAXS. Phases were identified using SAXS/WAXS and electron microscopy. L_α, fluid, lamellar phase; $P_{\beta'}$, ripple phase; $L_{\beta'}$, gel phase; Gel_1, gel phase composed of DPPC:4C12-PC16 19:1. This phase forms bilayers with macro-ripples. Gel_2, gel phase composed of DPPC:4C12-PC16 2:1. This phase forms flat bilayers. $_1H_{II}$, hexagonal phase; $_2H_{II}$, hexagonal phase composed of almost pure 4C12-PC16. X, additional nonlamellar phase only found by electron microscopy.

region as well, considering that electron microscopy shows evidence that a cubic phase may be present.

4.2. The gel phase range

Region 2 of the phase diagram contains a two-phase area. Fig. 6c provides direct evidence of the demixing into two bilayer domains, having an either flat or rippled appearance. Macroscopic gel–gel phase separation is not unusual and has been reported for a variety of binary mixtures, e.g. phosphatidylcholine and cholesterol [17], dimyristoyl- and distearoylphosphatidylcholines [18] and for mixtures phosphatidylcholines and diacylglycerols [19,20]. In general, the tendency for such segregation to take place increases with increasing disparity between the constituent lipids. The resulting differences in the respective mutual pair interactions hence favour contacts between identical molecules [21]. DPPC and 4C12-PC16 differ markedly in the hydrocarbon chain region, which is seen clearly if one considers the structures of the single components at identical temperatures: In the temperature range examined here, the four-chain lipid prefers a hexagonal fluid phase, whereas DPPC is in a gel phase bilayer at temperatures less than 42°C.

In contrast to macroscopic phase separations, the origin of the different microscopic structures of the demixed gel domains, namely bilayers with a macro-ripple superstructure versus flat membranes, is much more difficult to understand. What distinguishes both phases is the relative proportion of the individual lipid constituents. Low amounts of the four-chain lipid (5 mol%) cause macro-ripples whereas higher concentrations lead to a flattening of the bilayers. Understanding the reason for the formation of the macro-ripples is complicated by the fact that even for the pure phosphatidylcholine ripple phase no satisfactory model exists. Models based on thermodynamic considerations as well as statistical dynamic approaches (see [22] for a review) encounter difficulties when attempting to explain the nonsinusoidal profile and the varying periodicities of the ripples. A key factor in all models is the assumption that a chain headgroup cross-sectional area discrepancy causes problems in packing of the molecules, which are accommodated by forming the modulated structure.

Considering this, the incorporation of a second molecule in a gel phase phosphatidylcholine bilayer may relax or even increase these packing problems, probably depending on the molecular form and the concentration of the added molecule. In both cases a rearrangement of the lipid molecules within the bilayer is expected to take place. The reorganisation required to achieve a relaxation is effected by forming a different superstructure, e.g. macro-ripples. Which type of bilayer morphology is formed is likely to depend on the detailed molecular structure of the incorporated molecules. For instance, another solution to the packing problem may be the formation of interdigitated bilayers as demonstrated in mixtures of PC with ethanol [23] or asymmetric lipids [24].

The question remains whether a lipid with a propensity for nonlamellar structures is essential to form macro-ripples. Recent experiments with mixtures of palmitoyloleoylphosphatidylcholine and 40–80 mol% galactosylceramide, which form bilayers showing similar macro-ripples to those found in the present study, do not support this idea [25]. Neither lipid in pure form exhibits a ripple phase or a nonlamellar phase at this temperature. The phase diagram of the mixture indicates a gel–fluid coexistence region [26], which might indicate that rather than the tendency to form a nonlamellar phase a certain proportion of fluid chains must be present to allow a periodic tilting of the bilayer. This is particularly noteworthy, because 4C12-PC16 in pure form is also fluid at temperatures above $\sim$3°C. It could be that branched lipid with more or less fluid chains is localised in the crests and the valleys of the macro-ripples, thereby exerting a hinge function to enable the formation of the macro-ripples.

The other gel phase, Gel_2, contains a higher proportion of branched-chain lipid (33 mol%) and forms flat bilayers. This proportion of two DPPC molecules having a headgroup area slightly larger than the cross-sectional area of the chains ($T = 20$°C: $A_H \sim 46$ Å^2, $A_C \sim 40$ Å^2; [27]) and one four-chain lipid may be to provide an optimal balance between the average headgroup and cross-sectional area. Fig. 9 illustrates this idea on the basis of the molecular form concept.

Increasing the amount of four-chain lipid makes

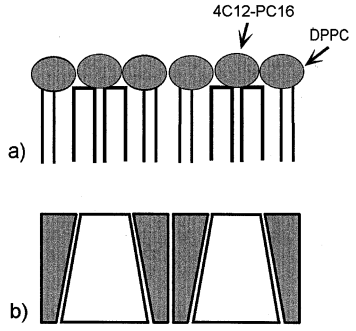

Fig. 9. (a) Schematic drawing of the suggested packing of lipid molecules in the bilayers formed by the Gel_2 phase. Two DPPC molecules are needed to compensate for the greater chain cross-sectional area of a branched-chain lipid. (b) Illustration according to the molecular form concept.

the binary system entering region 3 of the phase diagram, which is another two-phase region. In molecular terms this means that a gel bilayer containing more than one four-chain lipid per two DPPC molecules is no longer stable. The surplus branched-chain lipid segregates from the lamellar gel aggregates and forms a fluid hexagonal phase. During heating, the bilayer phase melts, but because of the increased area of the fluid chains, it remains unstable at temperatures above 35°C, and consequently, the lipid molecules will be incorporated into hexagonal cylinders. The incorporation of DPPC molecules into the $_1H_{II}$ phase reduces the spontaneous monolayer curvature and therefore enables a greater radius of curvature of these cylindrical micelles compared to those formed at lower temperatures. This is demonstrated convincingly by the shift of the hexagonal reflections towards lower angles upon heating (from 5.3 nm at 0°C to approx. 6.20 nm at 50°C).

4.3. The fluid phase range

The most conspicuous feature of the mixtures at temperatures above the liquidus line is the appearance of multiple X-ray reflections at low concentrations of the four-chain lipid (see Fig. 2b,d,f). Such multipeak profiles can arise from different structures.

Firstly, nonlamellar, e.g. hexagonal or cubic phases can create a complex set of scattering peaks. This possibility might be excluded, because the second order (although weak) of the reflections indicates that the peaks are of a lamellar type. Freeze-fracture micrographs obtained from samples quenched from the fluid phase did not show cubic or hexagonal structures, but patterned bilayers (Fig. 7c,d). The most reasonable explanation for this would be that the formation of macro-ripples could not be suppressed completely by the rapid quenching. Ultrarapid freezing experiments (not shown) using a propane-jet freezer, which provides a much higher freezing rate than manual plunging (20 000–30 000°/s compared to 2000–4000°/s, see [28]), however, resulted in structures of similar appearance. Therefore, it cannot be ruled out that the pattern is a genuine feature of fluid bilayers composed of DPPC and small amounts of the branched-chain lipid. The question whether some fluid lipid membranes show a periodic superstructure has been addressed recently [29], however currently no experimental method exists which is able to give an unambiguous answer. But even if we cannot exclude the possibility that the bilayer shows a superstructure in the fluid state it is unlikely that such a structure could cause multiple X-ray reflections of the type observed in this study.

The spacings of the reflections rather indicate two or more lamellar phases differing in lamellar repeat spacings. As the system is completely fluid at temperatures around 50°C, this would imply immiscibility of two fluid, lamellar phases. Direct evidence of such fluid–fluid phase separation has been found only rarely. Hinderliter et al. [30] reported the presence of two lamellar reflections in X-ray profiles obtained from phosphatidylserine/phosphatidylcholine samples in the fluid state. The first-order peaks found in the study presented here were at 6.9, 6.4 and $\sim$6.0/6.1 nm, which might indicate that three different fluid phases with different bilayer thicknesses may be present in the sample.

However, the multiple repeat periods can also be due to domains differing in the thickness of the water layer between the bilayers. This would again imply that the sample is phase separated into lipid domains that differ in their swelling properties. A similar effect was found recently in X-ray diffraction experiments of phosphatidylcholine suspensions containing alkali chloride ions [31]. These authors speculated that different water layers might be responsible for the appearance of several distinct lamellar reflections.

5. Conclusions

We analysed the phase behaviour of a fully hydrated binary mixture of DPPC with a branched-chain phosphatidylcholine. The binary system shows gel–gel immiscibility between 5 and 33 mol% of the branched-chain lipid. We suggest that the characteristic morphologies of these gel bilayer domains (rippled, flat) reflect the relaxation of a frustrated lipid packing state upon incorporation of the nonlamellar lipid into the PC bilayers. However, the nonlamellar propensity of the branched lipid does not seem to be of crucial importance for formation of macro-ripples. We suggest that, in general, the detailed structure of the second component like chain length or hydrophobicity determines the way gel phase bilayers of phosphatidylcholines adapt structurally to a new packing arrangement. In contrast, the transition to a hexagonal phase in the presence of proportions of branch chain lipid of about 33 mol% can be explained satisfactorily by the molecular form concept, which considers only the average form of the molecule.

Acknowledgements

We thank Ernie Komanschek for assistance in X-ray measurements in Daresbury and Gerd Rapp and Frank Richter for allowing us to perform X-ray measurements at DESY. We acknowledge the expert technical assistance of Ingemarie Herrmann and Renate Kaiser in preparing freeze-fracture replicas. This work was supported by the Deutsche Forschungsgemeinschaft, Teilprojekt A1 of the Sonderforschungsbereich SFB 197 and travel funds were provided by ARC project No. 804 of the British–German Academic Research Collaboration Programme.

References

[1] T. Kaneda, Microbiol. Rev. 55 (1991) 288–302.
[2] J.R. Silvius, M. Lyons, P.L. Yeagle, T.J. O'Leary, Biochemistry 23 (1985) 5388–5395.
[3] L. Rilfors, J.B. Hauksson, G. Lindblom, Biochemistry 33 (1994) 6110–6120.
[4] D. Schwarz, P. Kisselev, W. Pfeil, S. Pisch, U. Bornscheuer, R.D. Schmid, Biochemistry 36 (1997) 262–270.
[5] A.R.G. Dibble, A.K. Hinderliter, J.J. Sando, R.L. Biltonen, Biophys. J. 71 (1996) 1877–1890.
[6] P.J. Quinn, W.P. Williams, Biochim. Biophys. Acta 737 (1983) 223–266.
[7] J.N. Israelachvili, S. Marcelja, R.G. Horn, Q. Rev. Biophys. 13 (1980) 121–200.
[8] S.M. Gruner, M.W. Tate, G.L. Kirk, P.T. So, D.C. Turner, D.T. Keane, C.P. Tilcock, P.R. Cullis, Biochemistry 27 (1988) 2853–2866.
[9] D. Marsh, Biophys. J. 70 (1996) 2248–2255.
[10] R.N.A.H. Lewis, R.N. McElhaney, P.E. Harper, D.C. Turner, S.M. Gruner, Biophys. J. 66 (1994) 1088–1103.
[11] P. Nuhn, G. Brezesinski, B. Dobner, G. Förster, M. Gutheil, H.D. Dörfler, Chem. Phys. Lipids 39 (1986) 221–236.
[12] B. Rattay, G. Brezesinski, B. Dobner, G. Förster, P. Nuhn, Chem. Phys. Lipids 75 (1995) 81–91.
[13] I. Zimmermann, Struktur und Phasenverhalten von neuen Lipiden mit molekularen Modifizierungen im hydrophilen Bereich, Thesis, Martin-Luther-Universität, Halle-Wittenberg, 1997.
[14] W. Bras, G.E. Derbyshire, A. Devine, S.M. Clark, J. Cooke, B.E. Komanschek, A.J. Ryan, J. Appl. Cryst. 28 (1995) 26–32.
[15] W. Bras, G.E. Derbyshire, A.J. Ryan, G.R. Mant, P. Manning, R.E. Cameron, W. Mormann, J. Phys. (Paris) IV C8 3 (Suppl. I) (1993) 447–450.
[16] H.W. Meyer, B. Dobner, K. Semmler, Chem. Phys. Lipids 82 (1996) 179–189.
[17] T.P.W. McMullen, R.N. McElhaney, Biochim. Biophys. Acta 1234 (1995) 90–98.
[18] W. Knoll, K. Ibel, E. Sackmann, Biochemistry 20 (1981) 6379–6983.
[19] F. Lopez-Garcia, J. Villalain, J.C. Gomez-Fernandez, P.J. Quinn, Biophys. J. 66 (1994) 1991–2004.
[20] K. Semmler, H.W. Meyer, P.J. Quinn, Chem. Phys. Lipids 99 (1999) 155–167.
[21] W.L.C. Vaz, F.F. Almeida, Curr. Opin. Struct. Biol. 3 (1993) 482–488.
[22] J.M. Carlson, J.P. Sethna, Phys. Rev. A 36 (1987) 3359–3374.
[23] S.A. Simon, T.J. McIntosh, Biochim. Biophys. Acta 773 (1984) 169–172.
[24] S.W. Hui, J.T. Mason, C. Huang, Biochemistry 23 (1984) 5570–5577.
[25] R.E. Brown, W.H. Anderson, V.S. Kulkarni, Biophys. J. 68 (1995) 1396–1405.
[26] W. Curatolo, Biochim. Biophys. Acta 861 (1986) 373–376.
[27] G. Cevc, Phospholipids Handbook, Marcel Dekker, New York, 1993.
[28] T. Müller, S. Moser, M. Vogt, C. Daugherty, M.V. Pathasarathy, Scanning Microsc. 7 (1993) 1295–1310.
[29] R. Goetz, W. Helfrich, J. Phys. II France 6 (1997) 215–223.
[30] A.K. Hinderliter, J. Huang, G.W. Feigenson, Biophys. J. 67 (1994) 1906–1911.
[31] M. Rappolt, K. Pressl, G. Pabst, P. Laggner, Biochim. Biophys. Acta 1372 (1998) 389–393.